Mathematical Biosciences and Engineering, 16(4): 2492–2513.
DOI: 10.3934/mbe.2019125
Received: 24 December 2018
Accepted: 06 March 2019
Published: 22 March 2019

http://www.aimspress.com/journal/MBE

Research article

Human hands-and-knees crawling movement analysis based on time-varying synergy and synchronous synergy theories

Teng Li , Xiang Chen *, Shuai Cao , Xu Zhang and Xun Chen

Department of Electronic Science and Technology, University of Science and Technology of China, Hefei 230026, Anhui, P.R. China

*** Correspondence:** Email: xch@ustc.edu.cn.

Abstract: This paper aims to investigate human hands-and-knees crawling movement from the aspect of synchronous (SYN) and time-varying (TV) muscle synergy analysis. Nine healthy children and 11 children with cerebral palsy were recruited. During hands-and-knees crawling, surface electromyography (sEMG) signals from 12 main muscles of upper limbs and trunk were recorded, and muscle synergies were extracted based on TV synergy and SYN synergy theories. From the perspectives of repeatability, symmetry and similarity, the abilities of these two types of synergies to characterize crawling movement and to distinguish normal and abnormal crawling were explored. We found that: First, SYN synergy is better than TV synergy in depicting the body symmetry during crawling movement. However, TV synergy is more suitable than SYN synergy for distinguishing normal and abnormal crawling from the perspective of symmetry. Second, the abilities of SYN synergy and TV synergy in depicting the crawling repeatability are not comparable, and both have the potential to depict the crawling abnormality from the perspective of repeatability. Third, from the angle of inter-subject similarity, SYN synergy has the potential to describe the abnormal crawling pattern. However, the large individual differences suggest that TV synergy is a poor choice. This study provides a new way to analyze crawling movement from the perspective of neuromuscular control, and the research findings are meaningful for clinical assessment of abnormal crawling.

Keywords: crawling; cerebral palsy; synchronous synergy; time-varying synergy; surface electromyography

1. Introduction

Crawling is a kind of locomotion involving almost all limbs and trunk muscles and joints. For humans, there exist several crawling patterns, including hands-and-knees crawling, hands-and-feet crawling, creeping on belly, scooting, and combination styles [1]. Most toddlers crawl on hands-and-knees before they learn to walk [2]. According to inter-limb coordination, crawling can also be classified into pace-like, trot-like, and no-limb pairing types [3].

Using kinematic and electromyographic methods, much research on crawling movement has been conducted and reported [1–12]. Patrick et al. analyzed crawling on hands-and-knees along with hands-and-feet in healthy human adults and infants. These authors found that adults showed more flexible inter-limb coordination than infants and alternating patterns (e.g., trot-like) were predominant in infants [1,3]. To explore the connection of neural control mechanism between bipedal and quadrupedal in human adults, MacLellan et al. conducted a study on hands-foot crawling at different inclinations [9]. These authors mapped electromyography signals on the spinal cord and found that more remarkable sacral activities corresponding to typical features of bipedal walking emerged with more inclinations angles. To explore co-activation of antagonist muscles, Xiong et al. investigated the hands-and-knees crawling in healthy human infants and found that the co-activation index of upper limbs was higher than lower limbs, but the variability of co-activation pattern in upper limbs was less than in lower limbs [7,8]. Crawling in patients with cerebral palsy (CP) has also been researched. Bottos et al. found that crawling ability in CP children was positively correlated with the achievement of walking ability [12]. In summary, most studies on crawling focused on inter-limb coordination patterns and basic muscle co-activation analysis in healthy people, and few works involved the neuromuscular control characteristics or abnormal crawling patterns in patients such as CP.

On the other hand, muscle synergy theories have been widely applied to the study of neuromuscular control characteristics of human or animal locomotion. In general, muscle synergy theory hypothesizes that, for the sake of reducing redundancy or degree of freedom in locomotion control, muscle contractions generated by the central nervous system (CNS) can be represented by a combination of small basic activation patterns (or structures) [13–15], and that each activation pattern can be modulated spatially or temporally by corresponding coefficients. Based on different mathematic models and theory assumptions, three types of muscle synergies, including synchronous (SYN) synergy, time-varying (TV) synergy, and temporal synergy, have been proposed [16–18]. Among these, the mathematic models of temporal and SYN synergies are similar, and both of them belong to the time-invariant synergy approach [15]. Time-invariant synergy and time-varying synergy have different motion description abilities. For human elbow rotation movement, Enrico et al. extracted three temporal synergies, two SYN and two TV synergies respectively, and considered that the decompositions of each synergy method might represent a specific group of neurophysiological substrates [19].

The hypothesis of SYN synergy is that, in a specific synergy structure, all muscles were activated synchronously with constant relative activation level. Each synergy structure is correlated with an activation curve, which modulates the spatial-temporal activation level of the synergy [20–28]. Relevant studies have confirmed that SYN synergies could be regarded as physiological markers, reflecting abnormal statues of patients suffered from brain damage. Taking gait motion as an example, compared with healthy children, fewer SYN synergy number, abnormal synergy structures,

and lower synergy symmetry were found in CP children [20,21]. In a study on the target-matching movement of upper limbs, Roh et al. found that shoulder synergy structures in stroke participants were altered, and the alteration degree was related to abnormal matching performance [29]. What's more, abnormal patterns of SYN synergies were found in patients with cortical lesions, and the extent of abnormity was associated with severity of cortical damage and the duration of suffering from this disease [30]. SYN synergy analysis has also been adopted to analyze human crawling in related researches. For the crawling movement of healthy adults, Chen et al. extracted two synergies from each limb and found that one synergy was activated in stance phase and the other was activated in swing phase [6]. Gao et al. observed abnormal synergy activation in the hands-and-knees crawling movement of CP infants and attributed this abnormal activation to a damaged CNS [31].

Different from synchronous synergy, TV synergy theory assumes that the relative activation between muscles is time-varying [18,32]. Each TV synergy can be shifted in temporal domain through a time-delay coefficient, and adjusted in spatial domain by an amplitude coefficient. Time-varying synergy theory is another effective tool to explore neuromuscular control in the locomotion of animals and humans. D'Avella et al. found that TV synergies extracted from frog hindlimb of different kicking directions were highly similar [18]. Authors have also extracted four to five TV synergies from human fast-reaching movement and found those synergies could reconstruct sEMG patterns of reaching movements of different postures or loads [33].

Considering the research status of crawling movement and the potential abilities of muscle synergy theories in motion analysis, this paper investigated human hands-and-knees crawling movement from the aspect of muscle synergy analysis. With the goal of exploring the abilities of SYN and TV synergies in depicting crawling characteristics, healthy children and children with cerebral palsy were recruited as research subjects. Muscle synergies of the upper part of the body (including the upper arms and trunk) during hands-knees crawling were extracted based on TV synergy theory and SYN synergy theory. From the perspectives of repeatability, symmetry, and similarity, the abilities of these two types of synergies to characterize crawling movement and to distinguish normal and abnormal crawling were explored. The experimental results of this study shed light on how to properly use these two types of synergy analysis methods in the clinical assessment of abnormal crawling.

2. Materials and method

As shown in Figure 1, the main steps of this study include: 1) hands-and-knees crawling data acquisition; 2) data preprocessing; 3) TV and SYN synergies extraction, and 4) analysis of SYN and TV synergies in depicting crawling characteristics. Each step is introduced in detail below.

2.1. Hands-and-knees crawling data acquisition

2.1.1. Subjects

Nine healthy children (one female and eight males, 5.83 ± 2.38 years, TD group) and 11 children with cerebral palsy (four females and seven males, 4.68 ± 1.91 years, CP group) were recruited. None of the TD subjects had any history of neuromuscular diseases. All CP children were clinically diagnosed as cerebral palsy and could accomplish hands-and-knees crawling independently.

For the CP subjects, the exclusion criteria were: 1) individuals had undergone surgical therapy; 2) individuals could not understand the experiment instruction; 3) individuals with any other diseases that caused motor function impairment. Table 1 provides detailed information about all participants. The children's guardians were informed of the experimental protocol and provided written consent. The study was approved by the Ethics Review Committee of Anhui Medical University (No. PJ 2014-08-04).

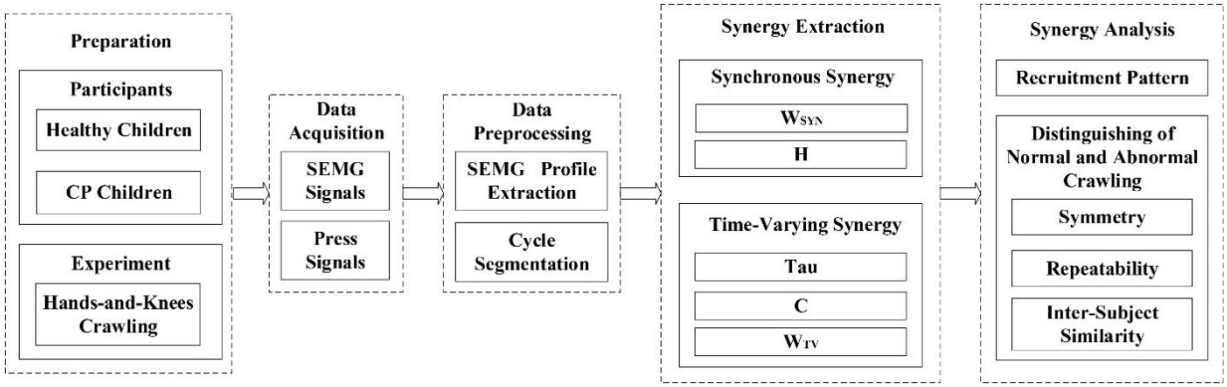

Figure 1. Flowchart of the main steps of the study**.**

Table1. Information of all participants.

Subjects	Gender	Age	Subjects	Gender	Age	Type	GMFCS
TD1	F	9.5	CP1	F	2	SP	2
TD2	M	2.5	CP2	F	4	AT	2
TD3	M	3	CP3	F	5	SP	*
TD4	M	3.5	CP4	F	7.5	SP	*
TD5	M	6	CP5	M	3	SP	*
TD6	M	6	CP6	M	3	SP	2
TD7	M	7	CP7	M	3.5	SP	1
TD8	M	7	CP8	M	3.5	SP	*
TD9	M	8	CP9	M	6	DY	3
			CP10	M	7	SP	4
			CP11	M	7	SP	*

* F: female, M: male, SP: spasticity, AT: ataxia, DY: dystonia, '*': data not obtained, GMFCS: Gross Motor Function Classification System. High GMFCS value means bad motor performance.

2.1.2. Crawling protocol

The protocols of the crawling experiment were as follows: (1) Participants crawl on a sponge mat along a straight line for at least ten cycles. (2) Participants crawl on hands-and-knees independently at a self-selected speed. Before the formal experiment, all children were instructed to practise until they were familiar with the crawling procedure.

2.1.3. Data acquisition

The muscle synergy of 12 main muscles of the upper limbs and trunk, which are associated with crawling, was investigated in this study. As shown in Figure 2, those muscles consist of biceps brachii (BB), triceps brachii (TB), trapezius (TR), anterior deltoid (AD), latissimus dorsi (LD), and erector spinae (ES). The placement of sEMG electrodes was based on the guideline of Development of Recommendations for SEMG Sensors and Sensor Placement Procedures [34]. To obtain high-quality sEMG signals, the selected muscles were cleaned and rubbed slightly with alcohol before the placement of the electrodes. Besides, to avoid the possible relative offsets between sEMG electrodes and the skin during crawling movement, sEMG electrodes were cling to the surface of muscles with kinesio taping. In addition to sEMG electrodes, two pressure sensors were placed at the flexor pollicis brevis of each hand to capture pressure signals for crawling cycle segmentation. During the crawling procedure, 12 channels of sEMG signals and two channels of pressure signals were collected synchronously through a home-made multi-channel data acquisition system (sEMG sensor: bipolar separating silver wire active electrode, pressure sensor: thin film piezoresistive pressure sensor. sEMG sampling rate: 2000Hz, and pressure sampling rate: 100Hz). To reduce the 50Hz power frequency interference to an acceptable degree, the data acquisition system was powered by lithium battery, and transmitted data to the laptop via USB. In addition, the laptop was powered by its own battery instead of 50Hz commercial power.

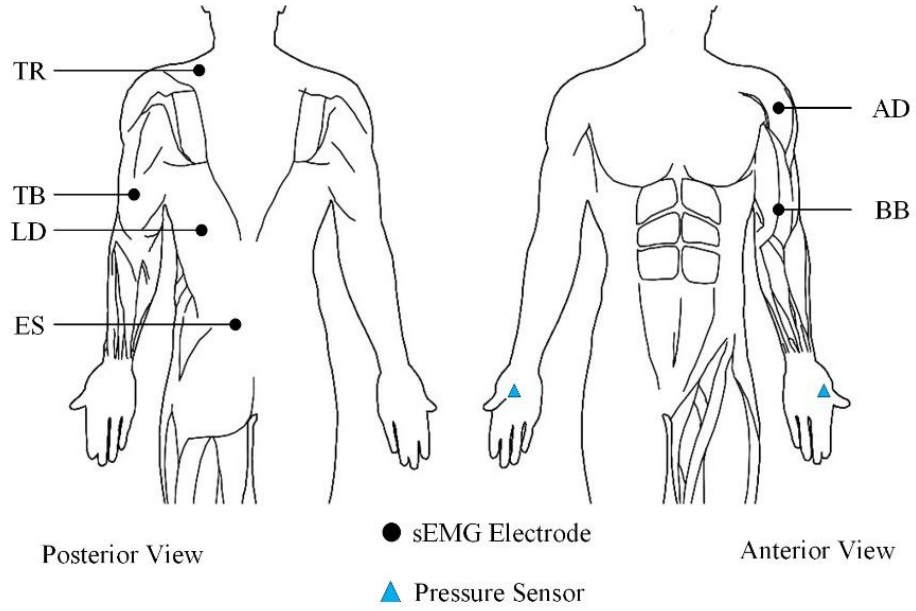

Figure 2. Placement of sensors.

2.2. Data preprocessing

Surface EMG signals were preprocessed through the following procedures: 1) high-pass-filtering by a Hamming window (length = 51) based finite impulse response filter (50th order, cutoff at 50Hz); 2) rectification; 3) low-pass-filtering with a Hamming window (length = 51) based finite impulse response filter (50th order, cutoff at 10Hz); and 4) normalizing to the maximum value of each channel.

2.3. Segmentation of crawling cycle, stance phase, and swing phase

For muscle synergy analysis, sEMG signals need to be segmented according to crawling cycles. One crawling cycle was defined as an interval starting from a ground-touching action of the left hand and ending with the next same action [3,6,9]. Because the pressure signal could reach a peak value rapidly once a ground-touching action happened, the ground-touching actions were detected by a windowed peak detecting algorithm [20] conducted on pressure signals. Pressure signals were also used to divide limb movements into a stance phase and swing phase in a crawling cycle. The stance phase was defined as an interval from the moment of limb touching the ground (peak pressure) to the moment of limb lifting off the ground (zero pressure). The swing phase was defined as an interval starting from the moment of limb lifting off the ground (zero pressure) and ending up with the moment of group-touching (peak pressure). Cycle length, namely the duration of a crawling cycle, was computed by the difference of two conterminous start points of the stance phase of the left hand.

To avoid disturbance and muscle fatigue, the middle five crawling cycles were selected for further analysis. Because the time durations of different crawling cycles were different even for the same subject, to unitize cycle length for facilitating the unification of programming, sEMG data in each cycle were resampled into 2000 points.

2.4. Muscle synergy extraction

2.4.1. Synchronous synergy

The Non-Negative Matrix Factorization (NNMF) algorithm was used to extract the SYN synergies [35,36]. In general, through the NNMF algorithm, a reconstructed sEMG signal matrix ($Mr_{m\times J}$, *m* means muscle number, *J* represents the length of one sEMG cycle) can be calculated by the product of synergy structure matrix ($W_{m\times n}$, *n* means synergy number) and synergy activation matrix ($H_{n\times J}$) as depicted in equation (1). According to related works [21,25,33], W represents the spatial activation level of a group of muscles during movements such as hands extending, gaiting and crawling [6,19,20,37]. H represents the temporal adjustment to the W and can depict how central nervous system adjust the activation level of muscle synergy over time [37]. Specifically, the NNMF algorithm starts with a random non-negative initialization of W and H, then iterates with W and H by gradient descent to improve the value of variability accounted for (VAF, ranges from 0 to 1) between Mr and the original sEMG matrix (Mo). Finally, the algorithm terminates when it reaches the threshold of the number of iterations or the threshold of VAF. Supposing the reconstructed matrix (Mr) could be calculated by equation (1), VAF can be expressed by equation (2).

$$\mathrm{Mr}_{\mathrm{m}\times\mathrm{J}} = \mathrm{W}_{\mathrm{m}\times\mathrm{n}} \times \mathrm{H}_{\mathrm{n}\times\mathrm{J}} \tag{1}$$

$$\mathrm{VAF} = 1 - (\mathrm{Mo} - \mathrm{Mr})^2/(\mathrm{Mo})^2 \tag{2}$$

In the theory of SYN synergy algorithm, synergy number is started at 1, and then the VAF under different synergy numbers are calculated.

2.4.2. Time-varying synergy

According to TV synergy theory [18,32,33], the original sEMG matrix M(t) could be decomposed into a synergy matrix, W, a time-delay (phase-shifting) coefficient vector, Tau, and an amplitude-adjustment coefficient vector, C, as shown in equation (3), in which *n* is the synergy number and *s* means the *s*-th cycle.

$$M_s(t) = \sum_{i=1}^{n} C_{si} \times W_i(t - Tau_{si}) \tag{3}$$

$$E^2 = \sum_{s=1}^{Nc} \sum_{t=1}^{J} \left\| M_s(t) - \sum_{i=1}^{n} C_{si} \times W_i\,(t - Tau_{si}) \right\|^2 \tag{4}$$

Taking the reconstruction error E^2 defined in equation (4) as the objective function, in which N_C represents the cycle number and J is the length of one sEMG cycle. The main steps of the TV synergy algorithm were shown in Figure 3(a), in which *a* means the number of iterations. In detail, the TV synergy algorithm can be described as two steps [18,36]:

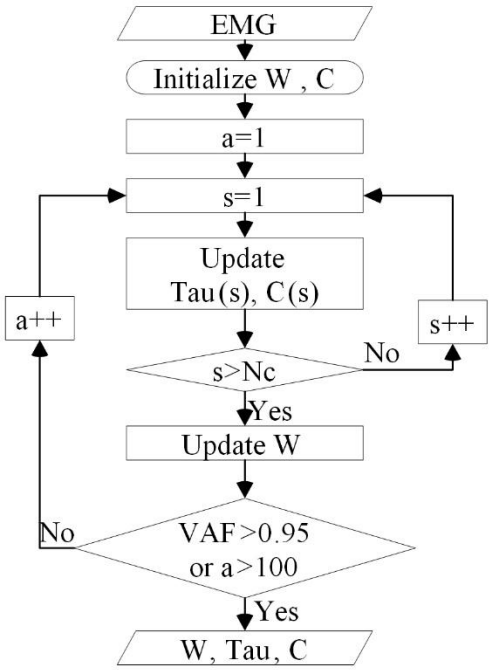

(a) Flowchart of TV algorithm

$$Wa = \left[W_1\ W_2 \ldots W_{J_S} \right]$$

$$Wb = \left[\overbrace{W_1\ W_2 \ldots W_{J_S}\ 0\,0 \ldots 0}^{\text{Col:J-Js}} \right]$$

$$Wc = \left[0\ \overbrace{W_1\ W_2 \ldots W_{J_S}\ 0\,0 \ldots 0}^{\text{Col=J-Js-1}} \right] (Tau = 1)$$

$$Wd = \left[\overbrace{W_2 \ldots W_{J_S}\ 0\,0 \ldots 0}^{\text{Col=J-Js+1}} \right] (Tau = -1)$$

(b) Nested Matching

Figure 3. TV algorithm.

Step 1: Initialize W and C with random positive values (ranges from 0 to 1);

Step 2: Minimize E^2 by iterating the following procedures: 1) For the *s*-th cycle, update Tau(s) by a 'Nested Matching' method, as described below, using the given W and C in the former step [32]; 2) For the *s*-th cycle, update C(s) using the non-negative least squares method, using W and Tau given in the former procedure [38]; 3) Repeat 1) and 2) until Tau and C of all cycles are updated; 4) Update W by the method of gradient descent; 5) Repeat the above four procedures until the algorithm reaches the threshold of number of iterations or the threshold of VAF.

The 'Nested Matching' method consists of five processes: 1) For the *i*-th synergy $Wa_{m\times Js}$ (*Js* means synergy length), enlarge Wa into a new matrix $Wb_{m\times J}$ ($Js \leq J$), as shown in Figure 3(b), in which *Col* corresponds to the number of columns. Then, shift elements in Wb along the row direction by Tau columns ($1\text{-}Js \leq Tau \leq J$) and replaced vacant columns of Wb with zeros to get Ws (Tau). For example, if Tau equals 1, Ws equals Wc, and if Tau equals -1, Ws equals Wd; 2) For all Tau values, calculate the similarity values between the original sEMG matrix (Mo) of the *s*-th cycle and Ws(Tau); 3) select the Ws and Tau corresponding to the highest similarity value, then multiply the selected Ws with C (given at the beginning of the first procedure of Step 2) to get $Wf_{m\times J}$; 4) Subtract Wf from Mo of the *s*-th cycle to get M_{NEW}; and 5) Replace Mo with M_{NEW}, then repeat the above four processes for the rest synergies.

In the theory of TV synergy algorithm, the synergy number is started at 2, and then the VAF under different synergy numbers are calculated.

2.4.3. Synergy similarity

For both SYN and TV synergy, synergy similarity was calculated based on the Pearson correlation coefficient (*r* value, ranges from -1 to 1), as shown in equation (5).

$$r = \frac{n\sum_i^n X_i Y_i - \sum_i^n X_i \sum_i^n Y_i}{\sqrt{n\sum_i^n X_i^2 - (\sum_i^n X_i)^2}\sqrt{n\sum_i^n Y_i^2 - (\sum_i^n Y_i)^2}} \quad (5)$$

For SYN synergy, the synergy structure or activation curve can be represented by a vector. Therefore, the similarity between any two synergy structures or between any two activation curves was represented by *r* values of two vectors. For TV synergy, each synergy structure was represented by a matrix ($W_{m\times Js}$, *m* means muscle number, *Js* means synergy length). To calculate the similarity between two TV synergy structures, the synergy matrix ($W_{m\times Js}$) was first reshaped into a vector ($W_{1,1}$,$W_{2,1}$,…, $W_{m,1}$, $W_{1,2}$, $W_{2,2}$, …, $W_{m,2}$, … , $W_{1,Js}$, $W_{2,Js}$, …,$W_{m,Js}$). Then, synergy similarity was represented by *r* values of two vectors.

2.4.4. Synergy co-activation

During crawling movement, two different synergies extracted from one body side may co-activate. In SYN analysis, to calculate the co-activation effect of two different synergies, co-activation coefficients of the whole crawling cycle (CAC_{ALL}), stance phase (CAC_{ST}) and swing phase (CAC_{SW}) are defined as equation (6), equation (7) and equation (8) respectively. In these equations, CA_{ALL}, $CA_{ST,}$ and CA_{SW} are the corresponding co-activation areas of the two synergies in the whole crawling cycle, stance phase, and swing phase respectively. H1 and H2 represent the

activation curves of the two synergies respectively. In TV analysis, co-activation coefficients of two different synergies are defined as equation (9). In this equation, Overlap means the length of the co-activation part of two synergies, and CycleLength means the length of one cycle.

$$\mathrm{CAC_{ALL}} = \mathrm{CA_{ALL}}/(\int \mathrm{H1} + \int \mathrm{H2} - \mathrm{CA_{ALL}}) \tag{6}$$

$$\mathrm{CAC_{ST}} = \mathrm{CA_{ST}}/(\int \mathrm{H1} + \int \mathrm{H2} - \mathrm{CA_{ALL}}) \tag{7}$$

$$\mathrm{CAC_{SW}} = \mathrm{CA_{SW}}/(\int \mathrm{H1} + \int \mathrm{H2} - \mathrm{CA_{ALL}}) \tag{8}$$

$$\mathrm{CAC_{TV}} = \mathrm{Overlap}/\mathrm{CycleLength} \tag{9}$$

2.4.5. Statistical analysis

An independent sample T-test was adopted for significant difference analysis of synergy parameters under different conditions. The threshold of significant difference was set to 0.05.

3. Results

3.1. Determination of synergy number

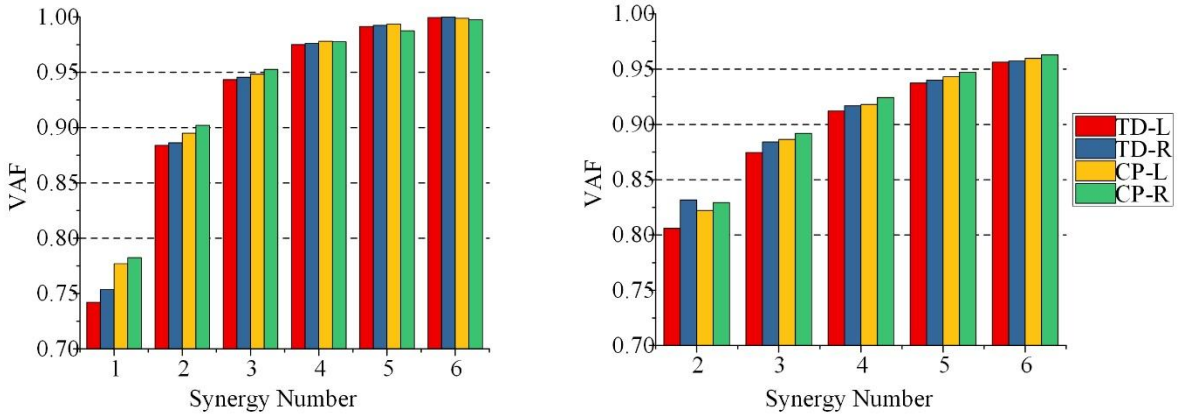

(**a**) SYN Synergy (**b**) TV synergy

Figure 4. Mean VAF values corresponding to the different number of synergies. L: left, R: right.

To determine the number of muscle synergies, 1~6 synchronous synergies and 2~6 time-varying synergies were extracted from all subjects. From Figure 4, which illustrates the mean VAF values of all subjects, we can observe that the VAF values of SYN synergy were higher than those of TV synergy when the synergy number was the same. For TV synergy, VAF values of two synergies

exceeded 0.80. In related research, VAF as 0.6~0.85 was usually used to determine the number of TV synergies [15,18,39]. Consequently, we thought two synergies were sufficient for TV synergy analysis of crawling movement. For SYN synergy, VAF as 0.92 or 0.95 or higher values usually were used to decide the synergy numbers in related works [20,25,37]. However, crawling was a rather complex movement with high degree of freedom, which may lower the ability of the predominant synergies in reconstructing the original sEMG signal, resulting in lower VAF. As shown in Figure 4 (a), for SYN synergy, the mean VAF values exceeded 0.85 when the synergy number was 2 and near to 0.95 when 3 synergies were extracted. In the data processing, we found that the third synergy had very low activation level and its structure varied greatly in different crawling cycles. We thought the third synergy may represent the difference between crawling cycles affected by individual or external factors. Considering that the study aimed to compare the ability of two synergy analysis methods in depicting crawling movement, the synergy number in SYN synergy analysis was also set to 2.

3.2. Extraction results of SYN synergy and TV synergy

3.2.1. SYN synergy

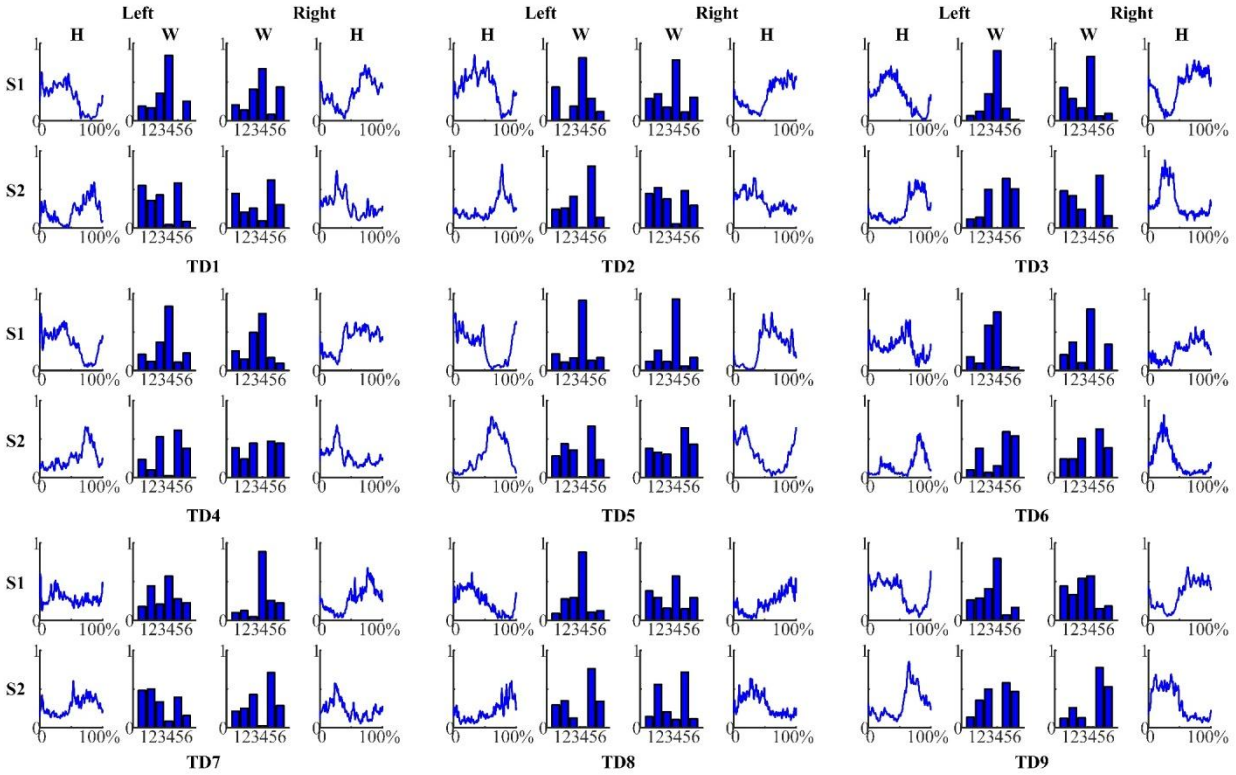

Figure 5. SYN synergy extraction results of TD subjects. W: synergy structure; H: activation curve; X-axis of H: the proportion of a crawling cycle; X-axis of W: 1: AD, 2: TR, 3: BB, 4: TB, 5: LD, 6: ES.

Figure 5 and Figure 6 show the SYN synergies extracted from the TD group (TD1~TD9) and CP group (CP1~CP11) respectively. For each side of each subject, two synergies were extracted from each cycle (one set of data) firstly, then the similar synergies in five cycles were averaged to get the

mean synergy. Each synergy (S) consisted of two parts: synergy structure (W) and activation curve (H). Following the definition given in the method section, at the beginning of a crawling cycle, the left upper limb first entered the stance phase, and the right upper limb was in the swing phase. Therefore, the first half of the H of the left side corresponded to the stance phase of the left upper limb, while the latter half corresponded to the swing phase. On the contrary, the first half of the H of the right side corresponded to the swing phase of the right limb, while the latter half corresponded to the stance phase. In this study, the synergies were classified according to the time they were activated (shown in H). S1 was activated mainly in the stance phase. Therefore, it was referred to as the stance synergy. S2 was activated mainly in the swing phase and was referred to as the swing synergy. A notable feature of the stance synergy (S1) was that the high activation level of the triceps brachii (TB) muscle. This was because the main function of the TB was to extend the forearm during the stance phase. Moreover, although the biceps brachii (BB) and the TB were a pair of antagonistic muscles, they were co-activated in the stance synergy. In the swing synergy (S2), activation amplitude of latissimus dorsi muscle (LD) was high due to its function of extending the arm, adducting the arm, and rotating the arm medially.

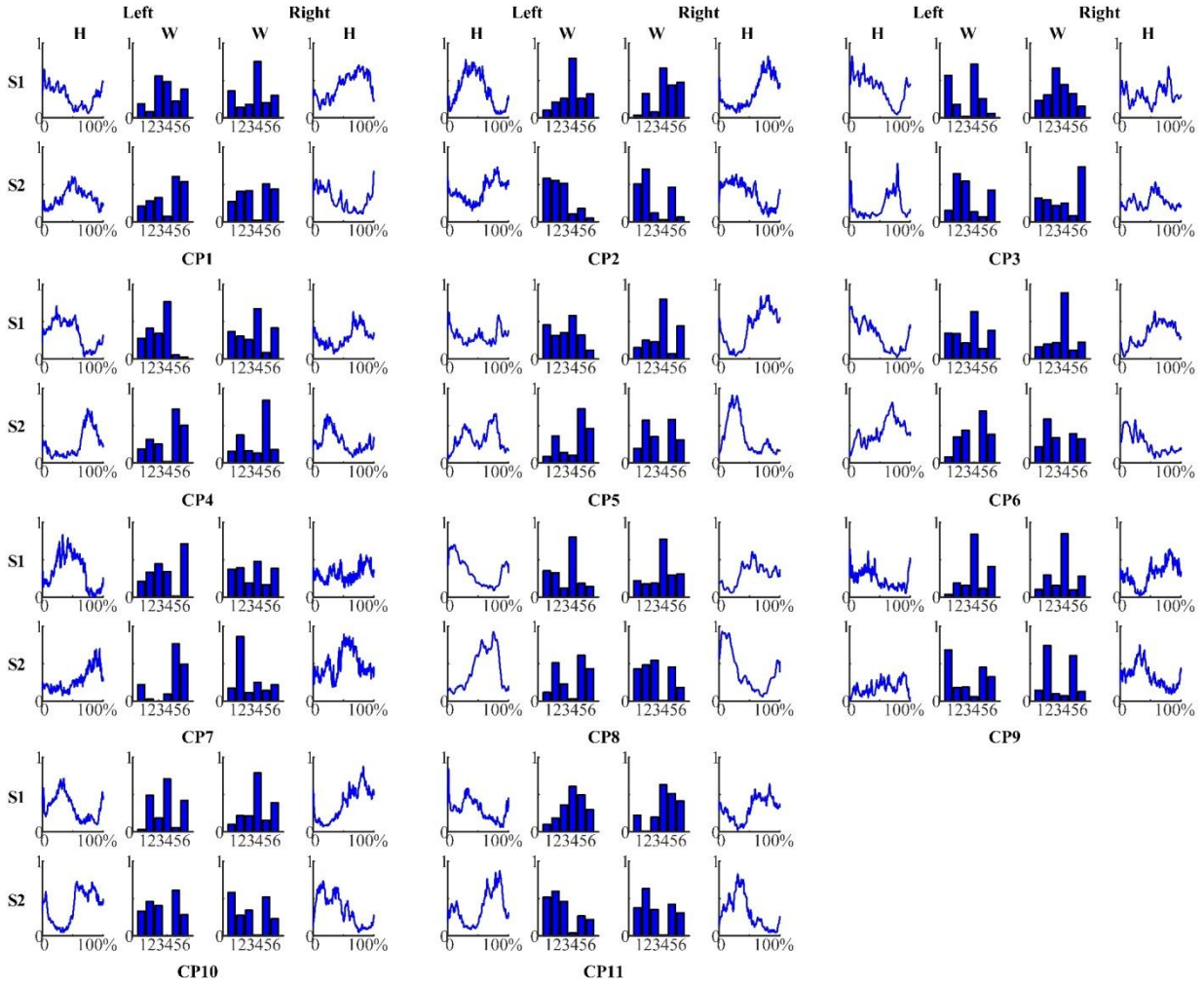

Figure 6. SYN synergy extraction results of CP subjects.

Figure 7 gives an example of co-activation (CA) between S1 and S2 of the left side. This indicated that the beginning of activation curves of stance synergy (H1) or swing synergy (H2) was ahead of the initiation of stance or swing phases. In particular, S1 was activated in advance of the stance phase (the endpoint of swing phase was also the starting point of the stance phase of the next crawling cycle), and the advanced phase was named the pre-stance phase (Pre-St). Similarly, a pre-swing phase (Pre-Sw) emerged in H2 since H2 reached a peak value before the beginning of the swing phase. Figure 8 shows the co-activation coefficients between S1 and S2 for all subjects. For both the TD group and CP group, the CAC_{ST} was significantly higher than CAC_{SW} on the same side ($p < 0.05$). Besides, the mean CAC_{ALL} of the CP group was higher than that of the TD group, although there was no significant difference ($p > 0.05$).

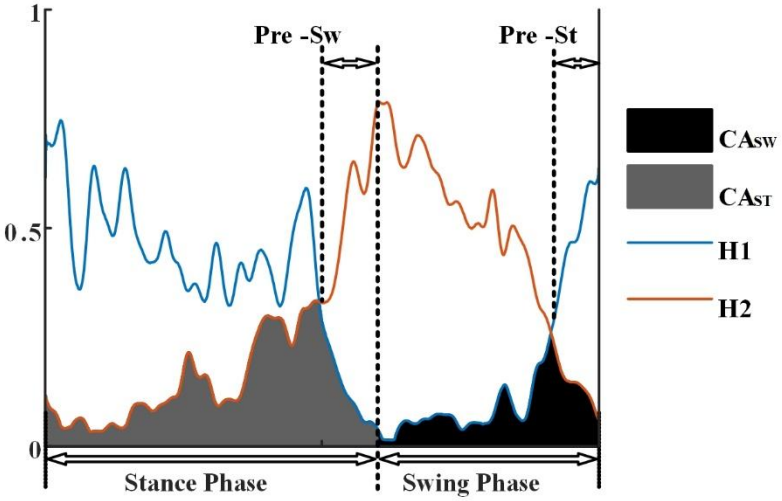

Figure 7. An example of SYN synergy co-activation. CAsw: CA of swing phase, CAst: CA of stance phase.

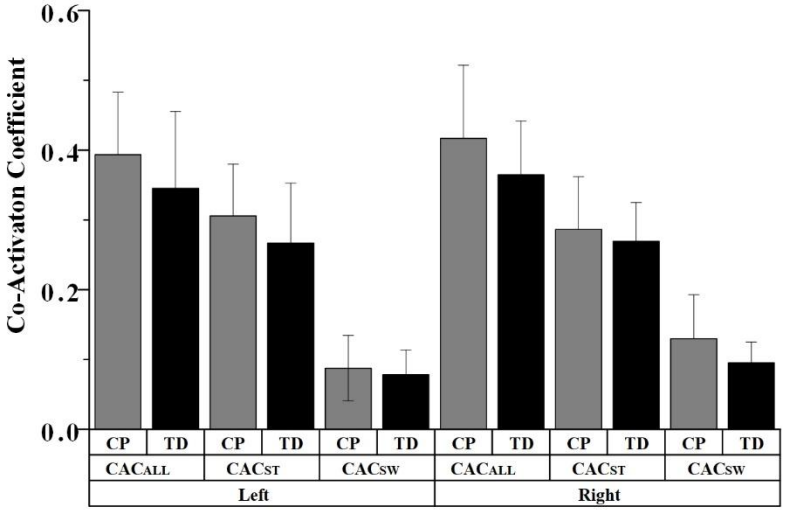

Figure 8. Co-activation of SYN synergy.

3.2.2. TV synergy

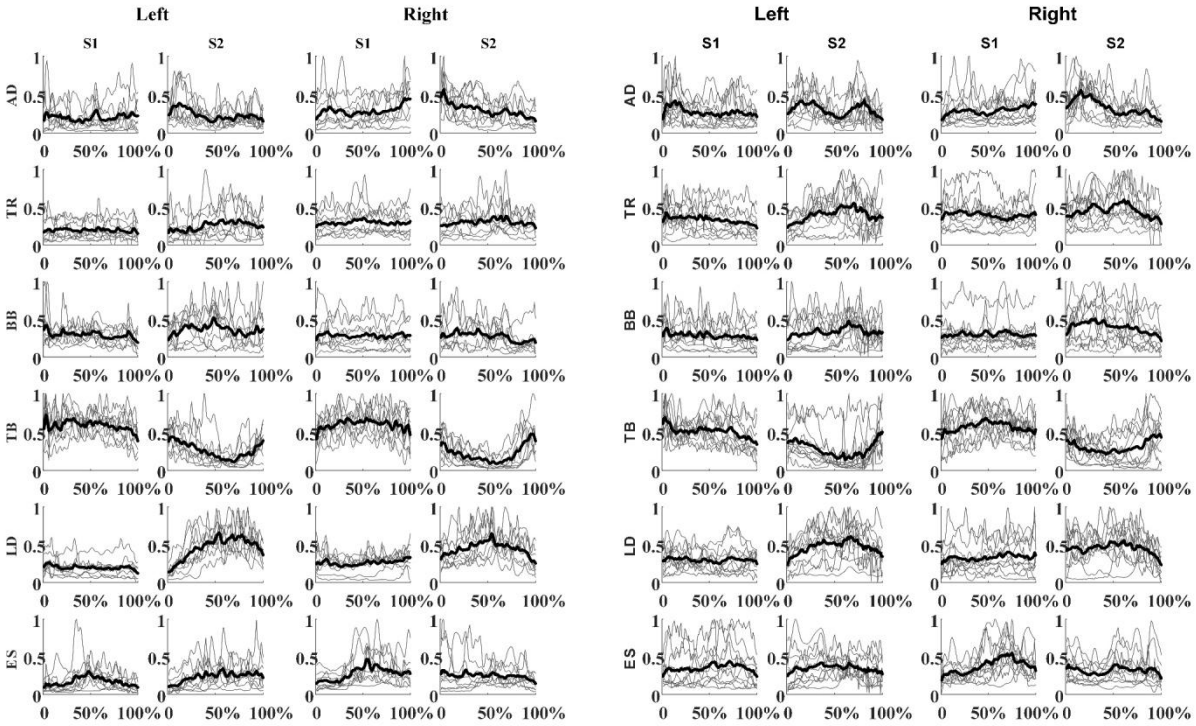

(**a**) TD group (**b**) CP group

Figure 9. TV synergy structures of all subjects. 0~100% in the X-axis represents the proportion of a synergy length. The thin gray line represents the activation curve of each subject, and the bold line is the averaged activation curve of all subjects.

For all subjects, two TV synergies were extracted from the left and right sides respectively. According to TV synergy theory, TV synergy structure was extracted from all five cycles. Therefore, in TV synergy, there was no definition of mean synergy structure. In each cycle, each synergy structure was accompanied with an amplitude adjustment coefficient and a time-delay coefficient. Table 2 shows the Tau values of the TV synergies of all subjects. The Tau values in this table were calculated from the following steps: First, for each subject, the Tau of five cycles of the same synergy were extracted and averaged. Second, the mean and standard deviation values of Tau of a group of subjects were calculated. Finally, the Tau values were represented as a percentage of cycle length. As shown in Table 2, for each side, the TV synergies were divided into two classes. For the left side, S1 and S2 were used to represent the classes that have 0%~20% and 40%~60% time-delay respectively. For the right side, S1 and S2 were used to represent the classes that have 40%~60% and 0%~20% time-delay respectively. As mentioned above, the crawling cycle was defined as starting from a ground-touching action of the left hand. Consequently, similar to SYN synergies, S1 and S2 were also called stance synergy and swing synergy respectively. Figure 9 shows the structures of the TV synergy extracted from all subjects. The characteristics of time-varying synergy were that the activation degree of each muscle changes along with the crawling time. Similar to SYN synergy, TB and LD muscles were dominantly activated in stance synergy and swing synergy respectively.

The co-activation coefficient of TV synergy (CAC_{TV}) was also calculated. For each subject, the CAC_{TV} of each cycle on each side was calculated first. Then, the average of five cycles on each side was calculated. For the TD group, the CAC_{TV} of the left side and right side were 0.02 ± 0.03 and 0.00 ± 0.00 respectively. For the CP group, the CAC_{TV} of the left side and right side were 0.02 ± 0.06 and 0.05 ± 0.09 respectively. There was no significant difference in CAC_{TV} between TD and CP groups in both the left side ($p = 0.95$) and the right side ($p = 0.10$). Based on the above results, we proposed that stance synergy and swing synergy of the same body side were relatively independent, having no tendency of co-activation.

Table 2. Tau values (Mean ± Std%) of all subjects.

Group	TD				CP			
Synergy	L_S1	L_S2	R_S1	R_S2	L_S1	L_S2	R_S1	R_S2
mean	1.12	49.17	51.43	1.34	1.52	49.69	46.75	1.75
std	7.32	6.95	6.24	6.09	10.98	12.78	11.74	10.68

* L means the left side, R means the right side.

3.3. Intra-subject synergy analysis for crawling movement

3.3.1. Synergy repeatability

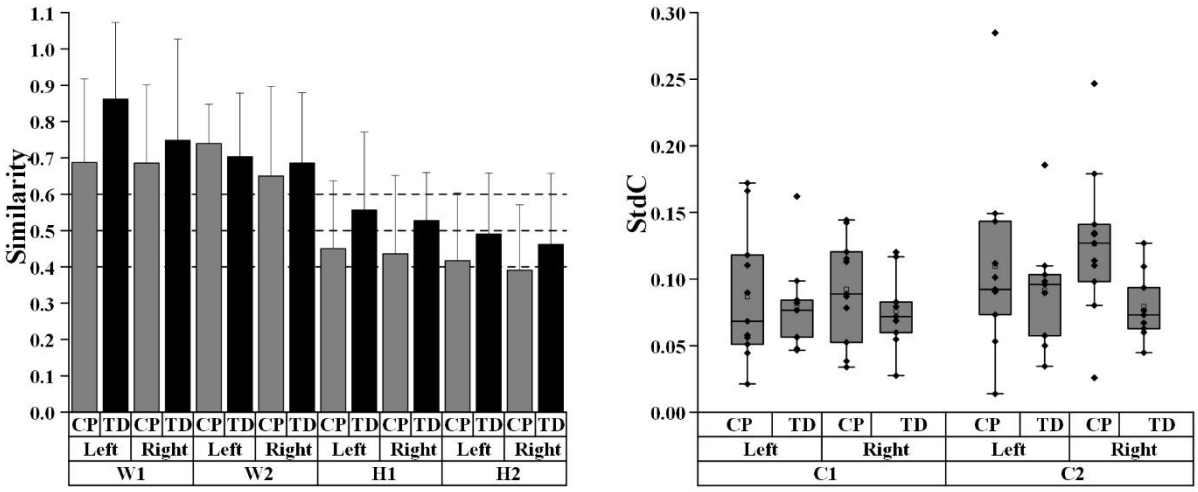

(**a**) SYN synergy (**b**) TV synergy

Figure 10. Intra-subject synergy repeatability.

For SYN synergy, the intra-subject synergy repeatability was explored from the similarity of both synergy structure (W) and activation curve (H) of five crawling cycles. The more similar the inter-cycle synergies, the higher the repeatability of the crawling movement. Figure 10(a) shows the intra-subject SYN synergy similarity of all subjects. For each subject, the synergy similarity value between every two cycles was calculated firstly, then the similarity values among the five cycles were averaged to represent repeatability. The mean and standard deviation of repeatability values in

each group was calculated. As shown in Figure 10(a), synergy structures had greater repeatability than activation curves in both the TD group and CP group. The mean repeatability in the TD group was larger than that in the CP group. However, there was no significant difference between these two groups ($p > 0.05$). Besides, for both the TD and CP groups, there was no significant difference in synergy repeatability between the same synergies of the left side and the right side or between stance synergy and swing synergy of the same side ($p > 0.05$).

For TV synergy, the intra-subject synergy repeatability was explored from the standard deviations of the amplitude adjustment coefficient (StdC) of five crawling cycles for each subject. Figure 10(b) illustrates the StdC values for both the TD group and CP group. Each point of each box represented the StdC of a subject. For each side, the mean StdC in the CP group was slightly higher than that in the TD group. The TD group had better consistency than the CP group with lower standard deviations (TD: Left side C1 = 0.08 ± 0.04, C2 = 0.09 ± 0.04, Right side C1 = 0.08 ± 0.03, C2 = 0.08 ± 0.03; CP: Left side C1 = 0.09 ± 0.05, C2 = 0.11 ± 0.07, Right side C1 = 0.09 ± 0.04, C2 = 0.13 ± 0.06). The StdC of C2 of the right side in CP was significantly higher than that in TD ($p = 0.03$). Besides, high StdC values (low repeatability) emerged in some CP subjects (e.g., StdC of C2 on the right side was 0.28 for CP1 and 0.25 for CP6).

3.3.2. Synergy symmetry

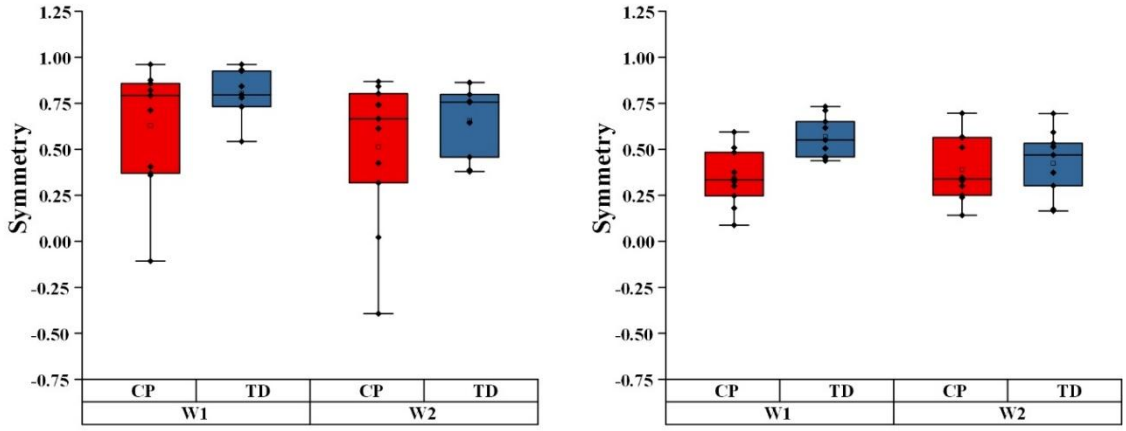

(**a**) SYN synergy (**b**) TV synergy

Figure 11. Synergy symmetry of all subjects.

Synergy symmetry was defined as the structure similarity of corresponding synergies between the left and right sides of a subject. Figure 11(a) illustrates the SYN synergy symmetry of all subjects, where each point in each box represented the symmetry value of a subject. The stance synergy had better symmetry than the swing synergy (W1: 0.80 ± 0.13; W2: 0.66 ± 0.20) in the TD group, and this phenomenon also emerged in the CP group (W1: 0.63 ± 0.33; W2: 0.51 ± 0.40). However, there was no significant difference between these two synergies in the TD group ($p = 0.08$) or CP group ($p = 0.47$). Although there was no significant symmetry difference between TD and CP subjects in both W1 ($p = 0.14$) and W2 ($p = 0.36$), the TD group had better consistency than the CP group, with lower standard deviations (TD: 0.13, 0.20; CP: 0.33, 0.40). Moreover, extremely low symmetry values ($r <$

0.2) were detected in some CP subjects.

Figure 11(b) illustrates TV synergy symmetry of all subjects, where each point in each box represented the symmetry value of a subject. Comparatively, the symmetry values of the two TV synergies in the TD group (W1: 0.57 ± 0.12, W2: 0.43 ± 0.18) were higher than those in CP group (W1: 0.34 ± 0.15, W2: 0.39 ± 0.17)). Moreover, the symmetry of W1 in the TD group was significantly higher than that in the CP group ($p = 0.001$). For both the TD and CP groups, the mean symmetry of the corresponding SYN synergy was higher than that in TV synergy. For instance, for the TD group, the mean symmetry of W1 was 0.80 for SYN synergy, but 0.57 for the TV synergy.

3.4. Inter-subject synergy similarity analysis for crawling movement

3.4.1. SYN synergy similarity

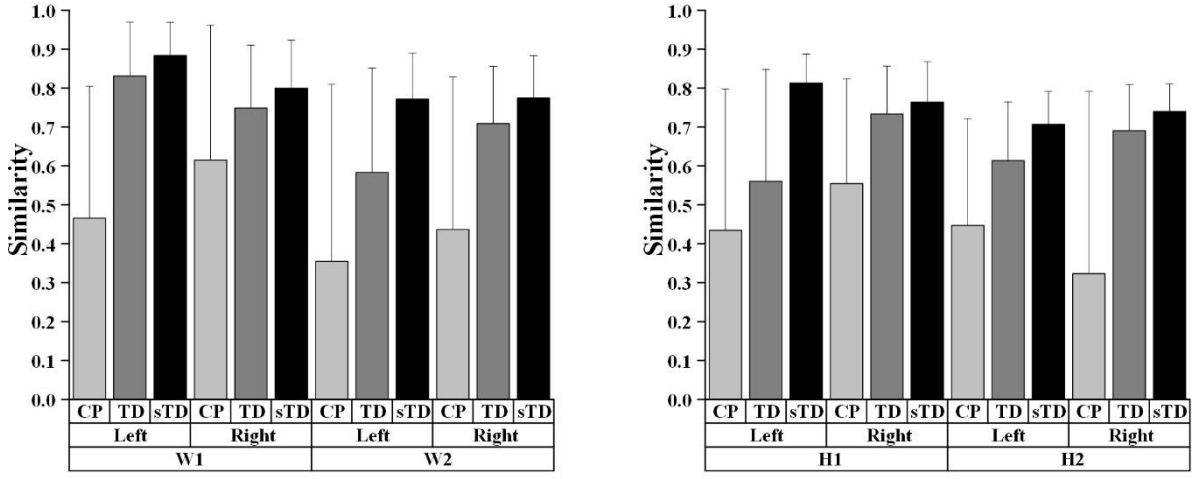

(a) W (b) H

Figure 12. Inter-subject SYN synergy similarity.

Figure 12 shows the SYN synergy similarity between subjects from the aspects of structure and activation curve. For each group, the similarity of corresponding synergies between every two subjects was first calculated, then the mean and standard deviation values were calculated. Comparing similarity values in the two groups, we found: first, for both W and H, the mean similarity values of CP group were significantly lower than those of TD group ($p < 0.05$); second, the inter-subject synergy similarity of some TD subjects was significantly higher than that of other subjects. These subjects with similarity greater than 0.80 were selected as a special TD (sTD) group, and the corresponding results were also given in Figure 12.

Because high synergy structure similarity existed in some TD subjects, typical synergy structure of stance synergy (T_W1) and that of swing synergy (T_W2) were extracted from the special TD group and shown in Figure 13. T_W1 was obtained by averaging the stance synergy structures in the special TD group. Similarly, T_W2 was obtained by averaging the swing synergy structures. Figure 14(a) gives the result of similarity analysis between SYN synergies of all subjects and the typical synergies. Each point in each box represented the similarity value between the synergy structure of

one subject and the corresponding typical synergy. From Figure 14(a), the following phenomenon could be observed: for TD subjects, the mean similarity values between W1 and T_W1 were high in both the left and right sides (left: 0.92, right: 0.88), and mean similarity values between W2 and T_W2 were relatively high (left: 0.78, right: 0.85). Some subjects showed relatively low structure similarity ($r < 0.6$) in swing synergy. For both stance synergy and swing synergy, there were no significant differences in structure similarity between the left side and right side (W1: $p = 0.42$, W2: $p = 0.33$) for CP subjects, mean similarity values between W1 and T_W1 (left: 0.69, right: 0.78) and those between W2 and T_W2 (left side: 0.58, right side: 0.48) were both relatively low. Extremely low similarity values ($r < 0.20$) emerged in some CP subjects. There was no significant difference between W1 and W2 of the same side (left: $p = 0.43$, right: $p = 0.41$), and there was also no significant difference in W1 or W2 when comparing the left and right sides (W1: $p = 0.40$, W2: $p = 0.56$).

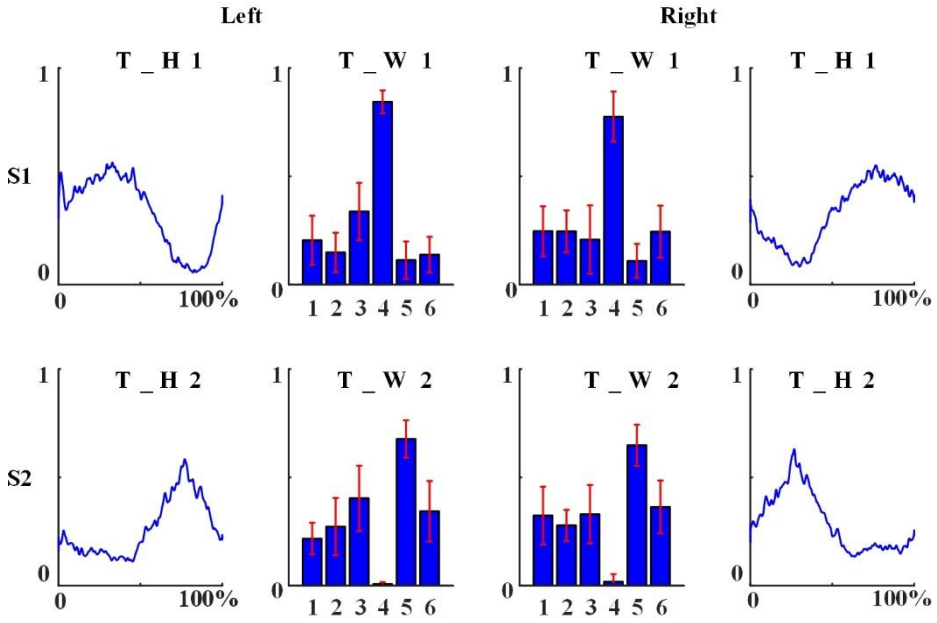

Figure 13. Typical SYN synergies extracted from sTD subjects. T_H: typical H, T_W: typical W.

Similarly, typical activation curve of stance synergy (T_H1) and that of swing synergy (T_H2) were also extracted from the special TD group and shown in Figure 13. Figure 14(b) reports the activation similarity analysis between SYN synergies of all subjects and the typical synergies. We found that the activation similarity of TD subjects was better than those of CP subjects with higher means and lower standard deviations. In detail, in TD subjects, the similarities of H1 and H2 are 0.77 ± 0.24 and 0.80 ± 0.11 for the left side, and 0.87 ± 0.09 and 0.85 ± 0.10 for the right side. In CP subjects, the mean similarities of H1 and H2 are 0.65 ± 0.31 and 0.67 ± 0.25 for the left side, and 0.74 ± 0.24 and 0.56 ± 0.48 for the right side. There was no significant difference in the similarity values between stance synergy and swing synergy on the same side or between the same synergy of different sides ($p > 0.05$).

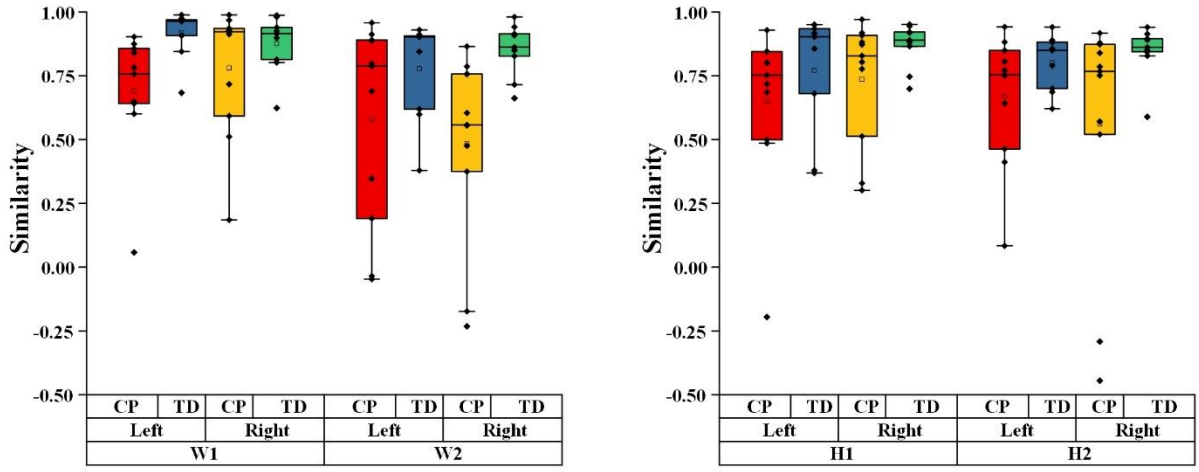

(**a**)W (**b**) H

Figure 14. The similarity between SYN synergies of each subject and the typical synergies.

3.4.2. TV synergy similarity

Table 3. Similarity (Mean ± Std) of TV synergy structure between subjects.

Synergy	L_W1		R_W1		L_W2		R_W2	
Group	TD	CP	TD	CP	TD	CP	TD	CP
Mean	0.47	0.34	0.58	0.31	0.37	0.32	0.39	0.28
Std	0.15	0.19	0.13	0.17	0.14	0.18	0.11	0.17

* L means the left side, R means the right side.

Table 3 shows the similarity values for TV synergy structures between subjects. For both the TD and CP groups, the similarity of the TV synergy was relatively low. For the CP group, the mean similarities of W1 were 0.34 for the left side and 0.31 for the right side, and the similarities of W2 were 0.32 for the left side and 0.28 for the right side. For the TD group, the mean similarities of W1 were 0.47 for the left side and 0.58 for the right side, and the mean similarities of W2 were 0.37 for the left side and 0.39 for the right side.

4. Discussion

Based on the premise that normal crawling has better symmetry, repeatability, and inter-subject similarity, healthy and cerebral palsy children were recruited in the study, and the abilities of SYN and TV synergies to characterize hands-and-knees crawling movement and to distinguish normal and abnormal crawling were explored in this study. The research results can be discussed as below.

Using both SYN and TV synergy extraction methods, during crawling movement, two synergies can be extracted from each side of the body. One is called the stance synergy and is activated mainly in the stance phase, and the other is called the swing synergy and is activated mainly in the swing phase. However, the recruitment patterns of these two types of muscle synergies are different. In SYN synergy analysis, a co-activation phenomenon between stance synergy and swing synergy was

detected. As shown in Figure 7, during the transition from stance to swing (Pre-Sw phase), the swing synergy was activated to provide the force to initiate swing movement. During the transition from swing to stance (Pre-St phase), stance synergy was activated to provide a force of extending limb and prepare the support of body weight for the upcoming stance phase. The phenomenon of co-activation between antagonist muscles was found in infants crawling previously. For instance, Xiong et al. found that the co-activation of antagonist muscles of the upper limb of the stance phase was lower than that of the swing phase [7]. Researchers have proposed that the co-activation between antagonist muscles is helpful for joint stability and movement accuracy during locomotion movement [8]. We also believe that the existence of co-activation of muscle synergies can make the conversion between motion modes smooth, avoiding or decreasing the possibility of muscle damage from rapid and drastic movement. In TV synergy analysis, however, stance synergy and swing synergy of the same body side were relatively independent, having no co-activation tendency.

Synergy symmetry was defined as the structure similarity of corresponding synergies between the left and right sides of a subject. In one SYN synergy research on walking [22], synergy symmetry between legs was found to be relatively lower in CP subjects than healthy subjects. In this study, when body symmetry was depicted with SYN synergy, the TD group has better consistency than the CP group with lower standard deviations, and extremely low symmetry values ($r < 0.2$) emerged in some CP subjects. This result indicates that SYN synergy can describe, to a certain extent, the crawling symmetry anomaly in CP children. However, there is no significant symmetry difference between the TD group and CP group. Regarding TV synergy, the symmetries in the TD group is higher than those in the CP group, and the symmetry of W1 in the TD group is significantly higher than that in the CP group. Reports addressing TV synergy symmetry are rare because EMG data is usually collected from one single body side [18, 19, 33, 38]. The results of this study show that TV synergy is more suitable than SYN synergy for distinguishing normal and abnormal crawling motion from the perspective of symmetry.

For SYN synergy, crawling repeatability was explored from the similarity values of both synergy structure and activation curve between crawling cycles. Synergy structures have better repeatability than activation curves in both the TD group and CP group. However, the TD group has better crawling repeatability than the CP group when the similarity of activation curves is used as the index. For TV synergy, crawling repeatability was explored from the standard deviations of amplitude adjustment coefficients (StdC) of crawling cycles for each subject. The TD group has better consistency in repeatability than the CP group with lower standard deviations. The repeatability of the swing phase of the right side in the CP group was significantly lower than that in the TD group, and some CP subjects show extremely low crawling repeatability. Consequently, TV synergy and SYN synergy both have the potential to depict the crawling abnormality from the perspective of repeatability.

Regarding the inter-subject similarity, for SYN synergy, the CP group was significantly lower than the TD group in both synergy structure and activation curve. Specifically, typical synergies extracted from a special TD group have certain application potentials in evaluating crawling anomalies. In other words, the degree of deviations in the structure and activation pattern between CP subjects' synergies and the typical synergies could reflect the degree of crawling abnormality in CP subjects. Consequently, SYN synergy has the potential to describe the abnormal crawling pattern. However, for TV synergy, although the TD group has relatively higher similarity values than the CP group, the similarity was very low in both groups. The large individual differences indicate that the

TV synergy is not suitable for distinguishing normal and abnormal crawling patterns from the aspect of inter-subject similarity.

5. Conclusion

Here we investigated muscle synergy analysis of crawling movement. Specifically, SYN and TV muscle synergies theory were adopted for the analysis of human hands-knees crawling. Taking healthy children and children with cerebral palsy as research subjects, the abilities of these two synergies to characterize crawling movement from the perspectives of symmetry, repeatability, and inter-subject similarity were explored, and the experimental results demonstrated that those two types of synergies have their own merits and drawbacks in distinguishing normal and abnormal crawling. Considering the great potential in revealing the neuromuscular control strategy of muscle synergy analysis, these findings are also of great significance for understanding the underlying control mechanism of the CNS during normal and abnormal crawling movements.

Acknowledgments

We appreciate the children and their guardians for participating in this research. We also thank the doctors, therapists, and nurses for their assistance in the experiment. Finally, we would like to thank our team members and tutors for their help in data collection and article modification. This work was supported by the National Nature Science Foundation of China (grant numbers: 61671417 and 61431017).

Conflict of interest

The authors declare no conflict of interest in this paper.

References

1. S. K. Patrick, J. A. Noah and J. F. Yang, Developmental constraints of quadrupedal coordination across crawling styles in human infants, *J. Neurophysiol*., **107** (2012), 3050–3061.
2. M. Hildebrand, Symmetrical gaits of primates, *Am. J. Phys. Anthropol.*, **26** (1967), 119–130.
3. S. K. Patrick, J. A. Noah and J. F. Yang, Interlimb coordination in human crawling reveals similarities in development and neural control with quadrupeds, *J. Neurophysiol.*, **101** (2009) 603–613.
4. M. J. MacLellan, G. Catavitello and Y. P. Ivanenko, et al., Planar covariance of upper and lower limb elevation angles during hand-foot crawling in healthy young adults, *Exp. Brain Res.*, **235** (2017), 3287–3294.
5. S. Ma, X. Chen and S. Cao, et al., Investigation on inter-limb coordination and motion stability, intensity and complexity of trunk and limbs during hands-knees crawling in human adults, *Sensors*, **17** (2017), 1–15 .
6. X. Chen, X. C. Niu and D. Wu, et al., Investigation of the intra- and inter-Limb muscle coordination of hands-and-knees crawling in human adults by means of muscle synergy analysis, *Entropy*, **19** (2017), 1–15.

7. Q. L. Xiong, X. Y. Wu and N. Xiao, et al. The variability of co-activation pattern of antagonist muscles in human infant crawling, *Annual International Conference of the IEEE Engineering in Medicine and Biology Society*, (2016), 331–334.
8. Q. L. Xiong, X. Y. Wu and N. Xiao, et al. Antagonist muscle co-activation of limbs in human infant crawling: A pilot study, *Annual International Conference of the IEEE Engineering in Medicine and Biology Society*, (2015), 2115–2118.
9. M. J. MacLellan, Y. P. Ivanenko and G. Cappellini, et al., Features of hand-foot crawling behavior in human adults, *J. Neurophysiol.*, **107** (2012), 114–125.
10. S. Gallagher, J. Pollard and W. L. Porter, Locomotion in restricted space: Kinematic and electromyographic analysis of stoopwalking and crawling, *Gait Posture*, **33** (2011), 71–76.
11. K. E. Adolph, B. Vereijken and M. A. Denny, Learning to crawl, *Child Dev.*, **69** (1998): 1299–1312.
12. M. Bottos, M. L. Puato and A. Vianello, et al., Locomotion pattern in cerebral palsy syndromes, *Dev. Med. Child Neurol.*, **37** (1995), 883–899.
13. M. Hirashima and T. Oya, How does the brain solve muscle redundancy? Filling the gap between optimization and muscle synergy hypotheses. *Neurosci. Res.*, **104** (2016), 80–87.
14. S. Aoi and T. Funato, Neuromusculoskeletal models based on the muscle synergy hypothesis for the investigation of adaptive motor control in locomotion via sensory-motor coordination, *Neurosci. Res.*, **104** (2016), 88–95.
15. A. d'Avella and F. Lacquaniti, Control of reaching movements by muscle synergy combinations. *Front. Comput. Neurosci*, **7** (2013), 1–7.
16. V. C. K. Cheung, A. d'Avella and M. C. Tresch, et al., Central and sensory contributions to the activation and organization of muscle synergies during natural motor behaviors, *J. Neurosci.*, **25** (2005), 6419–6434.
17. Y. P. Ivanenko, R. E. Poppele and F. Lacquaniti, Five basic muscle activation patterns account for muscle activity during human locomotion. *J. Neurophysiol.*, **556** (2004), 267–282.
18. A. d'Avella, P. Saltiel and E. Bizzi, Combinations of muscle synergies in the construction of a natural motor behavior. *Nat. Neurosci.*, **6** (2003), 300–308.
19. E. Chiovetto, B. Berret and I. Delis, et al., Investigating reduction of dimensionality during single-joint elbow movements: a case study on muscle synergies, *Front. Comput. Neurosci.*, **7** (2013), 1–12.
20. L. Tang, F. Li and S. Cao, et al., Muscle synergy analysis in children with cerebral palsy, *J. Neural. Eng.*, **12** (2015), 1–12.
21. K. M. Steele, A. Rozumalski and M. H. Schwartz, Muscle synergies and complexity of neuromuscular control during gait in cerebral palsy, *Dev. Med. Child Neurol.*, **57** (2015), 1176–1182.
22. A. S. Oliveira, L. Gizzi and D. Farina, et al. Motor modules of human locomotion: influence of EMG averaging, concatenation, and number of step cycles. *Front. Hum. Neurosci.*, **8** (2014), 1–9.
23. E. Zwaan, J. G. Becher and J. Harlaar, Synergy of EMG patterns in gait as an objective measure of muscle selectivity in children with spastic cerebral palsy, *Gait Posture*, **35** (2012), 111–115.
24. K. Czupryna and J. Nowotny, Changes of kinematics parameters of pelvis during walking under the influence of means facilitates treatment of cerebral palsied children, *Ortop. Traumatol. Rehabil.*, **14** (2012), 453–465.

25. N. Dominici, Y. P. Ivanenko and G. Cappellini, et al., Locomotor primitives in newborn babies and their development, *Science*, **334** (2011), 997–999.
26. G. T. Oviedo and L. H. Ting, Subject-specific muscle synergies in human balance control are consistent across different biomechanical contexts, *J. Neurophysiol.*, **103** (2010), 3084–3098.
27. M. C. Tresch and A. Jarc, The case for and against muscle synergies. *Curr. Opin. Neurobiol.*, **19** (2009), 601–607.
28. L. H. Ting and J. L. McKay, Neuromechanics of muscle synergies for posture and movement. *Curr. Opin. Neurobiol.*, **17** (2007), 622–628.
29. J. Roh, W. Z. Rymer and E. J. Perreault, et al, Alterations in upper limb muscle synergy structure in chronic stroke survivors, *J. Neurophysiol.*, **109** (2013), 768–781.
30. V. C. K. Cheung, A. Turolla and M. Agostini, et al., Muscle synergy patterns as physiological markers of motor cortical damage, *Proc. Natl. Acad. Sci. U.S.A.*, **109** (2012), 14652–14656.
31. Z. Gao, L. Chen and Q. Xiong, et al. Degraded synergistic recruitment of sEMG oscillations for cerebral palsy infants crawling, *Front. Neurol.*, **9** (2018), 1–12.
32. A. d'Avella and M. C. Tresch. Modularity in the motor system: Decomposition of muscle patterns as combinations of time-varying synergies, *Adv. Neural. Inf. Process. Syst.*, (2002), 141–148.
33. A. d'Avella, A. Portone and L. Fernandez, et al., Control of fast-reaching movements by muscle synergy combinations, *J. Neurosci.*, **26** (2006), 7791–7810.
34. H. J. Hermens, B. Freriks and C. D. Klug, et al., Development of recommendations for SEMG sensors and sensor placement procedures, *J. Electromyogr. Kinesiol.*, **10** (2000), 361–374.
35. D. D. Lee and H. S. Seung, Learning the parts of objects by non-negative matrix factorization, *Nature*, **401** (1999), 788–791.
36. Q. Huang, D. Tao and X. Li, et al., Parallelized Evolutionary Learning for Detection of Biclusters in Gene Expression Data, *IEEE/ACM Trans Comput. Biol. Bioinform.*, **9** (2012), 560–570.
37. L. Tang, X. Chen and S. Cao, et al., Assessment of Upper Limb Motor Dysfunction for Children with Cerebral Palsy Based on Muscle Synergy Analysis, *Front. Hum. Neurosci*, **11** (2017), 1–13.
38. A. D'Avella and E. Bizzi, Shared and specific muscle synergies in natural motor behaviors, *Proc. Natl. Acad. Sci. U.S.A.*, **102** (2005), 3076–3081.
39. S. A. Overduin, A. d'Avella and J. Roh, et al., Modulation of muscle synergy recruitment in primate grasping, *J. Neurosci.*, **28** (2008), 880–892.

AIMS Press